Supplementary materials

High - pressure polymorphs of the ferroan dolomite: possible host structures for carbon in the lower mantle

Naira S. Martirosyan[1,2,3*], Ilias Efthimiopoulos[1#], Sandro Jahn[2], Sergey S. Lobanov[1], Richard Wirth[1], Hans-Josef Reichmann[1], Monika Koch-Müller[1]

[1] GFZ German Research Centre for Geosciences, Telegrafenberg, 14473 Potsdam, Germany

[2] Institute of Geology and Mineralogy, University of Cologne, Zülpicher Str. 49b, 50674 Köln, Germany

[3] Bayerisches Geoinstitut, University of Bayreuth, Universitätsstraße 30, 95447 Bayreuth, Germany

#Present address: Max-Planck-Institut für Eisenforschung GmbH, Max-Planck-Str. 1, 40237 Düsseldorf

*Corresponding author: naira.martirosyan@uni-bayreuth.de

Tables:

Table S1. Unit cell parameters of the studied samples at atmospheric pressure (Dol-I structure, SG R-3).

Figure captions:

Fig. S1 X-ray diffractions and structures of dolomite polymorphs. Structure visualizations are from (Merlini et al 2012, 2017; Binck et al., 2020).

Fig. S2. Raman spectra of Ank19 (xFe = 0.19) collected with NaCl pressure medium.

Fig. S3. Raman spectra of Ank19 (xFe = 0.19) collected with Ar pressure medium.

Fig. S4. Example of the Voigt fitting of the Dol-Ib (9.6 GPa) and Dol-II (18.1 GPa) Raman spectra within the 150-450 cm^{-1} frequency range. Spectra were collected for Ank19 (xFe = 0.19) in Ar pressure medium. Green dots – experimental data, blue line – theoretical curve.

Fig. S5. Raman spectra of Ank19 (xFe = 0.19) collected in the experiment with Ne pressure medium.

Fig. S6. Raman spectra of Ank23 (xFe = 0.23) collected upon compression up to 27 GPa showing the transition from Dol-I to Dol-II. *(a)* low-frequency part with magnified intensities and (*b)* high-frequency part of the spectra.

Fig. S7. Raman spectra of Ank23 (xFe = 0.23) showing the transition from Dol-II to Dol-IIIc.

Fig. S8. Raman spectra of Dol-IIIc and Dol-II. Data is from Efthimiopoulos et al., (2017, 2019)

Fig. S9 The XRD patterns of Ank23 (xFe = 0.23) collected at different pressures. Dashed lines show position of Ne peak. Arrows point at the new peaks.

Fig. S10 The XRD patterns of Ank40 (xFe = 0.40) collected at different pressures. Dashed lines show position of Ne peak. Arrows point at the new peaks.

Fig. S11 The XRD patterns of Ank64 (xFe = 0.64) collected at different pressures. Dashed lines show position of Ne peak. Arrows point at the new peaks.

Fig. S12 The XRD patterns of Ank40 and Ank23. Calculated XRD of Dol-IIIc and IIIb (red patterns) are given for comparison.

Fig. S13 The Rietveld refinement of the Ank40 XRD pattern obtained at 41.1 GPa, using Dol-IIIb (upper figure, wR=19.9%) and Dol-IIIc (lower figure, wR=42.5%) models in combination with Ne. The experimental curve is indicated with crosses. The green and blue lines represent the calculated XRD and the difference curve, respectively. The Bragg positions of Dol-IIIb or IIIc (in black) and Ne (in blue) are marked by ticks.

Fig. 14. The Le Bail refinements of the XRD patterns of the (a) Ank5 (P = 38 GPa), (b) Ank2 (P = 41 GPa), and (c) Ank4 (P = 44 GPa), collected at the highest experimental pressure of each run (λ = 0.2906 Å, T = 300 K). Open circles are the experimental data, red lines – the Le Bail refinements, and blue lines – the difference curves. The corresponding structural parameters are listed in Table 1. Asterisks mark the Bragg peaks of the Ne PM.

Fig. S15. Results of the Raman spectroscopy analyses of the Ank19 before and after heating at 42GPa.

Table S1. Unit cell parameters of the studied samples at atmospheric pressure (Dol-I structure, SG R-3).

Sample	Formula	a, Å	c, Å	V, Å
Ank40	$Ca_{0.99}(Mg_{0.55}Fe_{0.40}Mn_{0.06})(CO_3)_2$	4.83(5)	16.12(1)	326.47(5)
Ank23	$Ca_{0.97}(Mg_{0.77}Fe_{0.23}Mn_{0.03})(CO_3)_2$	4.81(2)	16.08 (2)	322.70(1)
Ank64	$Ca_{0.99}(Mg_{0.33}Fe_{0.64}Mn_{0.05})(CO_3)_2$	4.84(5)	16.20 (2)	328.19(5)

Note. Ank19 sample was analyzed only with Raman spectroscopy method, as it exhibits an almost identical Raman spectroscopic behavior as Ank23.

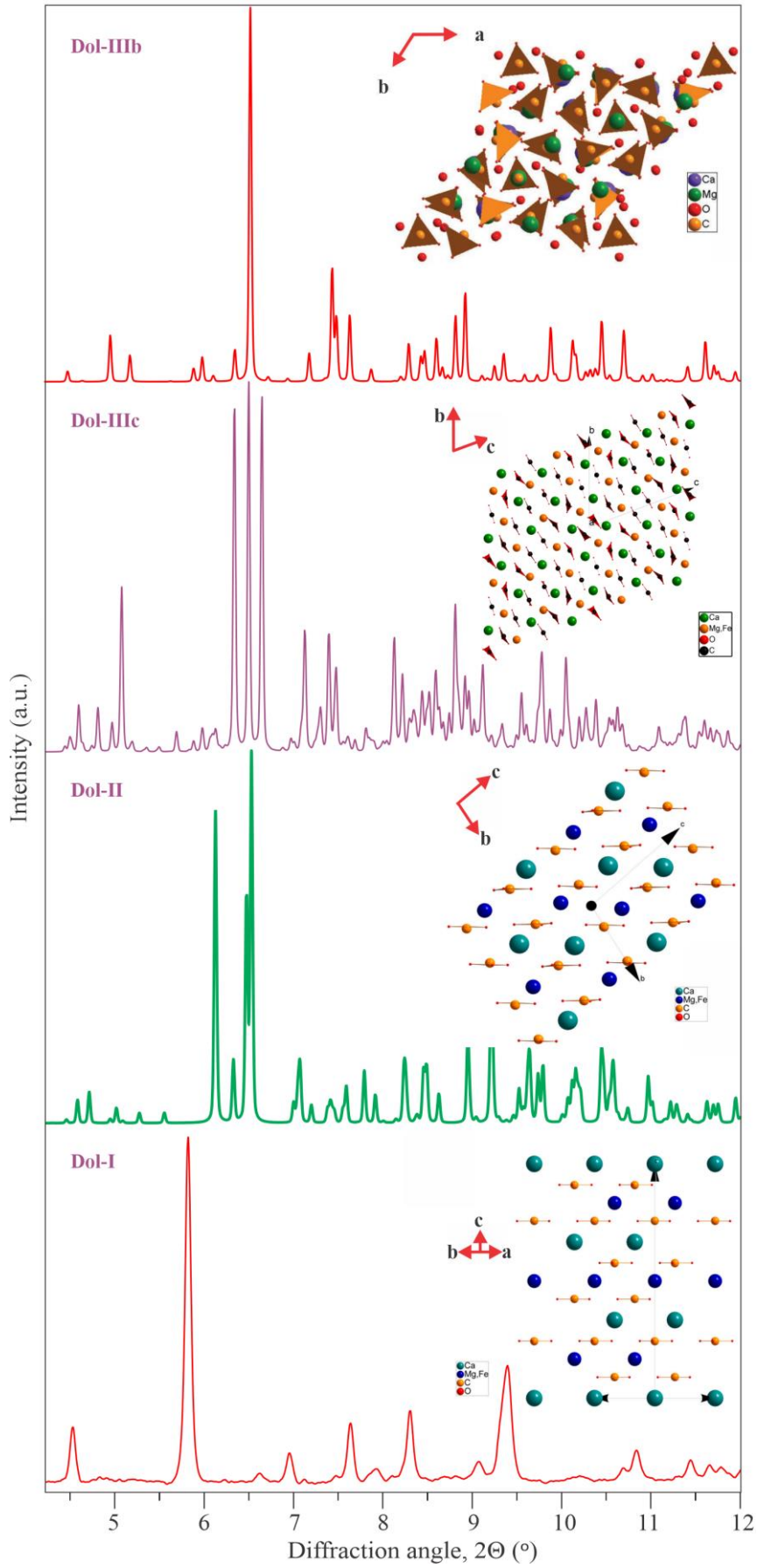

Fig. S1 X-ray diffractions and structures of dolomite polymorphs. Structure visualizations are from (Merlini et al 2012, 2017; Binck et al., 2020).

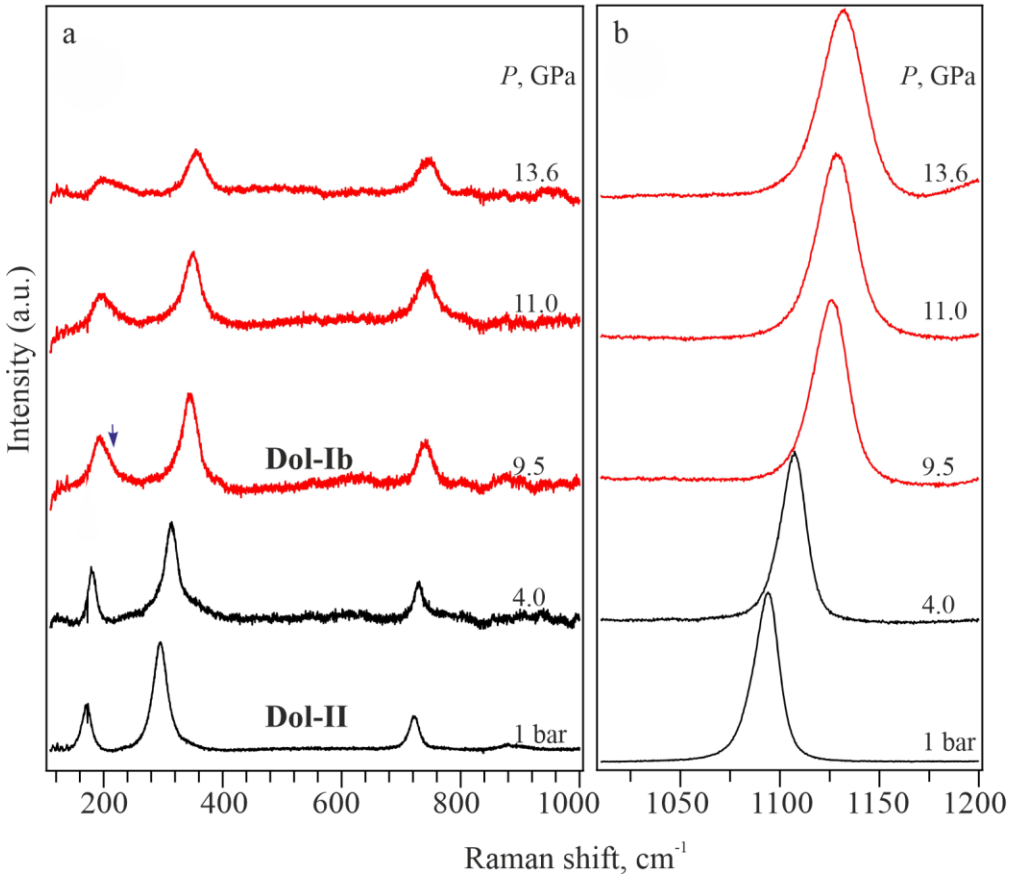

Fig. S2. Raman spectra of Ank19 (xFe = 0.19) collected with NaCl pressure medium.

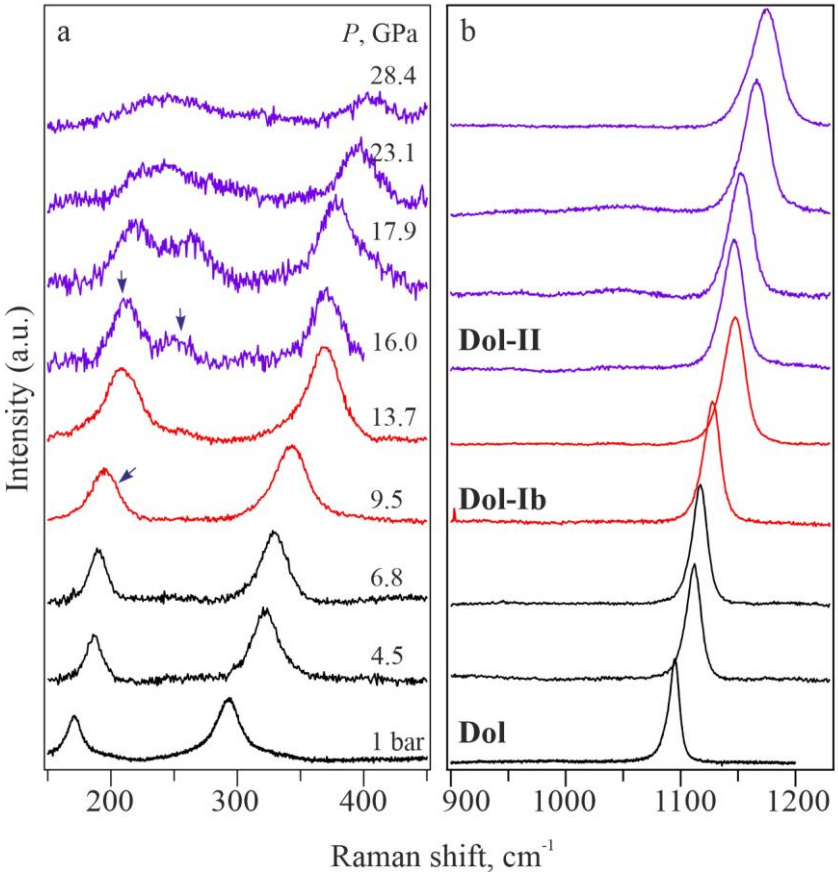

Fig. S3. Raman spectra of Ank19 (xFe = 0.19) collected with Ar pressure medium.

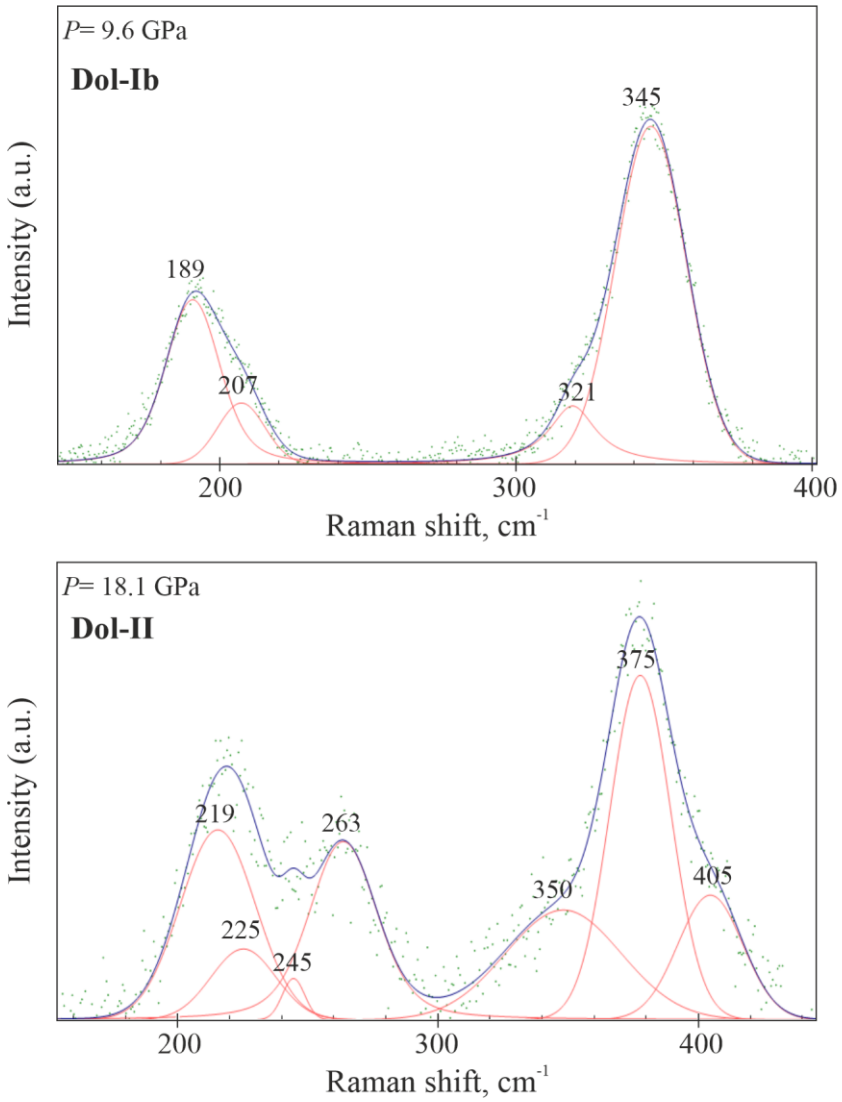

Fig. S4. Example of the Voigt fitting of the Dol-Ib (9.6 GPa) and Dol-II (18.1 GPa) Raman spectra within the 150-450 cm^{-1} frequency range. Spectra were collected for Ank19 (xFe = 0.19) in Ar pressure medium. Green dots – experimental data, blue line – theoretical curve.

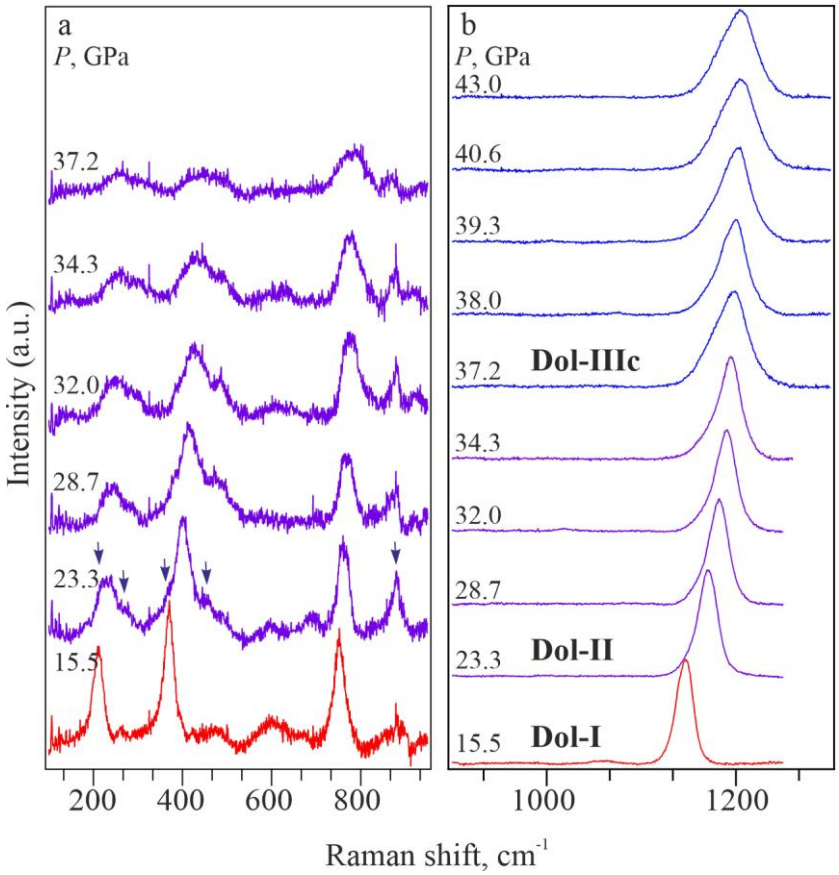

Fig. S5. Raman spectra of Ank19 (*xFe* = 0.19) collected in the experiment with Ne pressure medium.

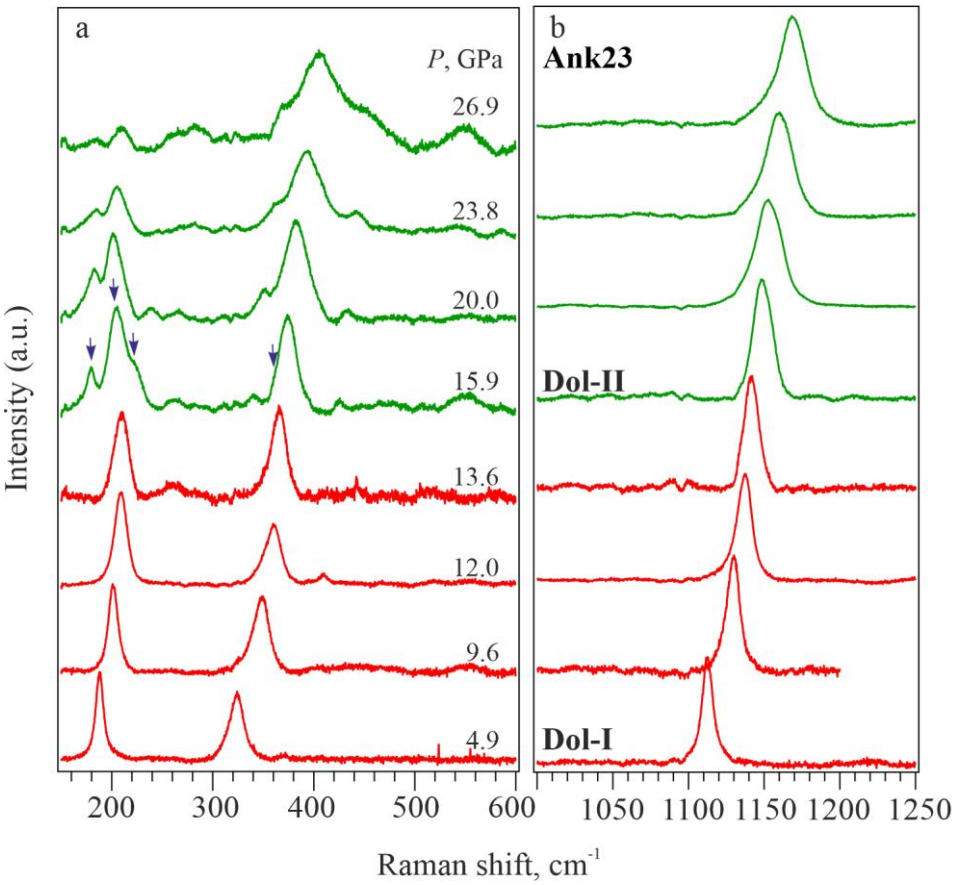

Fig. S6. Raman spectra of Ank23 (*xFe* = 0.23) collected upon compression up to 27 GPa showing the transition from Dol-I to Dol-II. *(a)* low-frequency part with magnified intensities and (*b)* high-frequency part of the spectra.

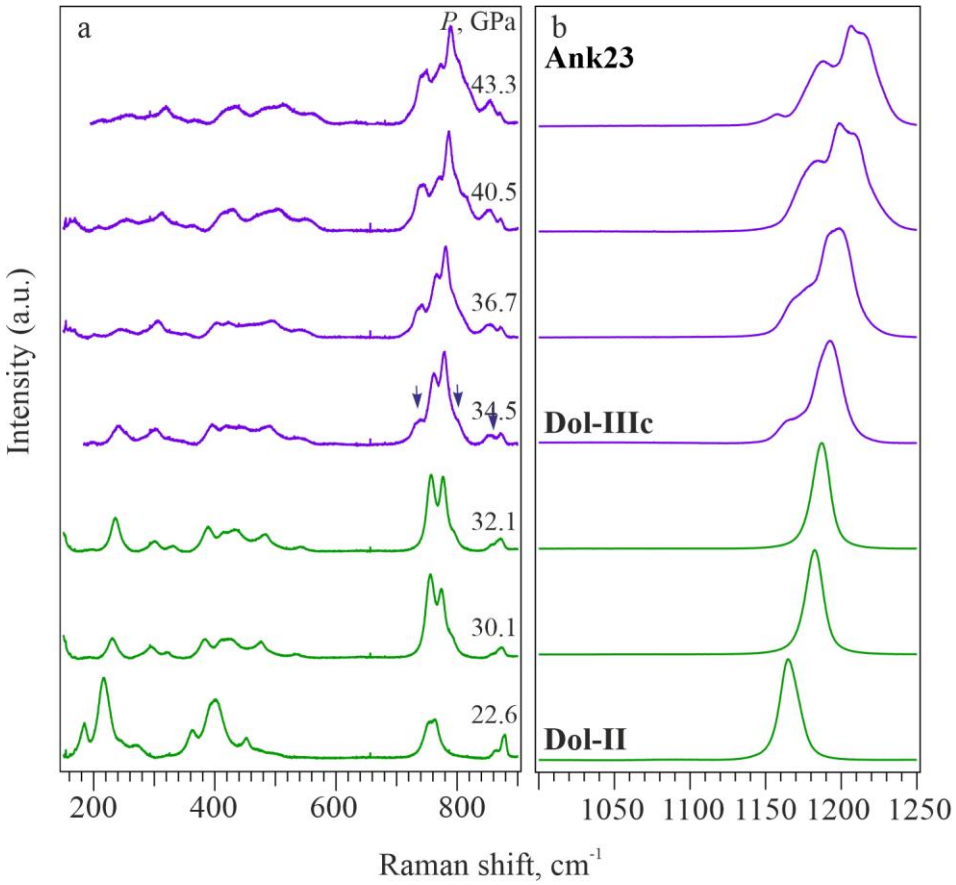

Fig. S7. Raman spectra of Ank23 (*xFe* = 0.23) showing the transition from Dol-II to Dol-IIIc.

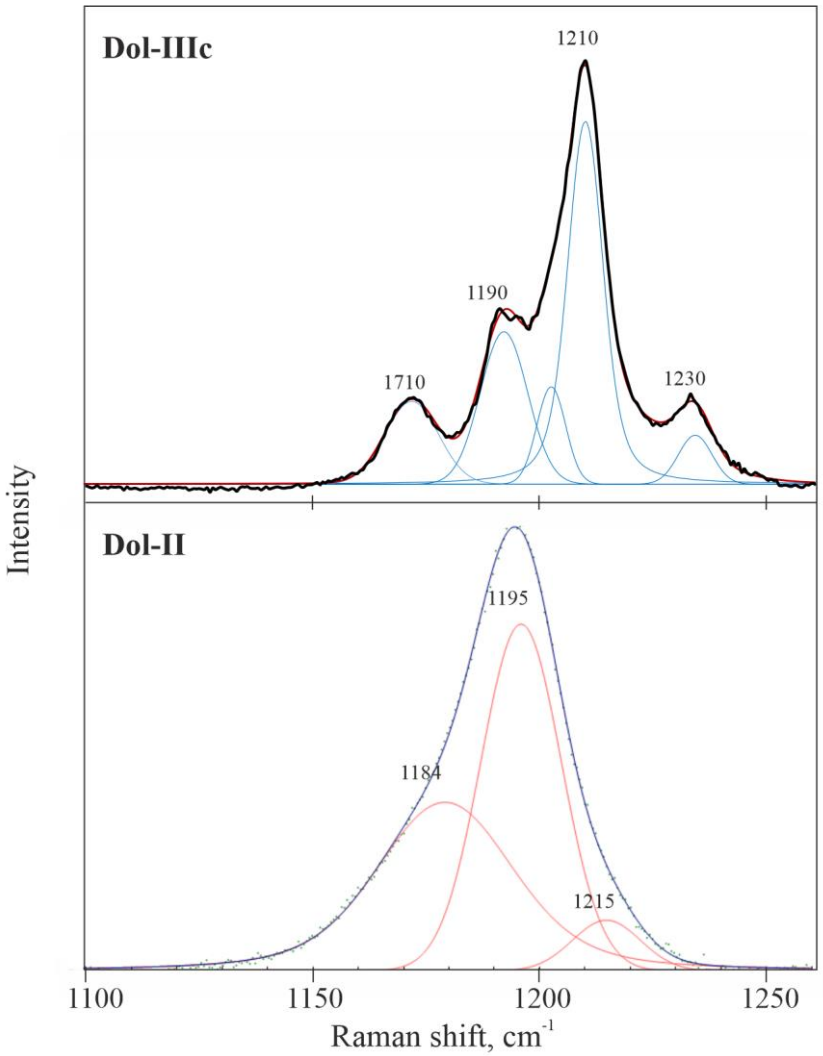

Fig. S8. Raman spectra of Dol-IIIc and Dol-II. Data is from Efthimiopoulos et al., (2017, 2019)

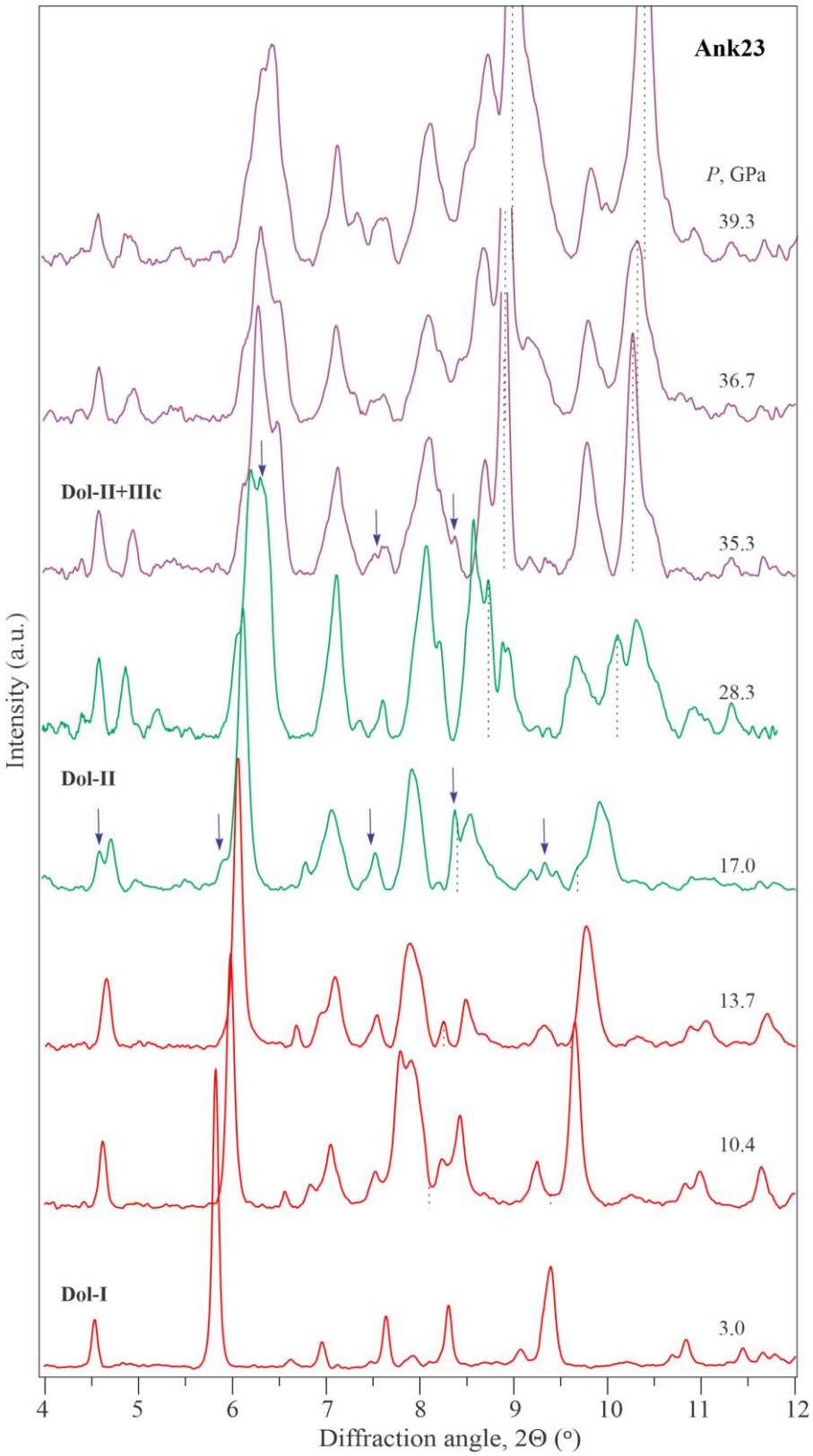

Fig. S9 The XRD patterns of Ank23 (*xFe* = 0.23) collected at different pressures. Dashed lines show the position of Ne peak. Arrows point at the new peaks.

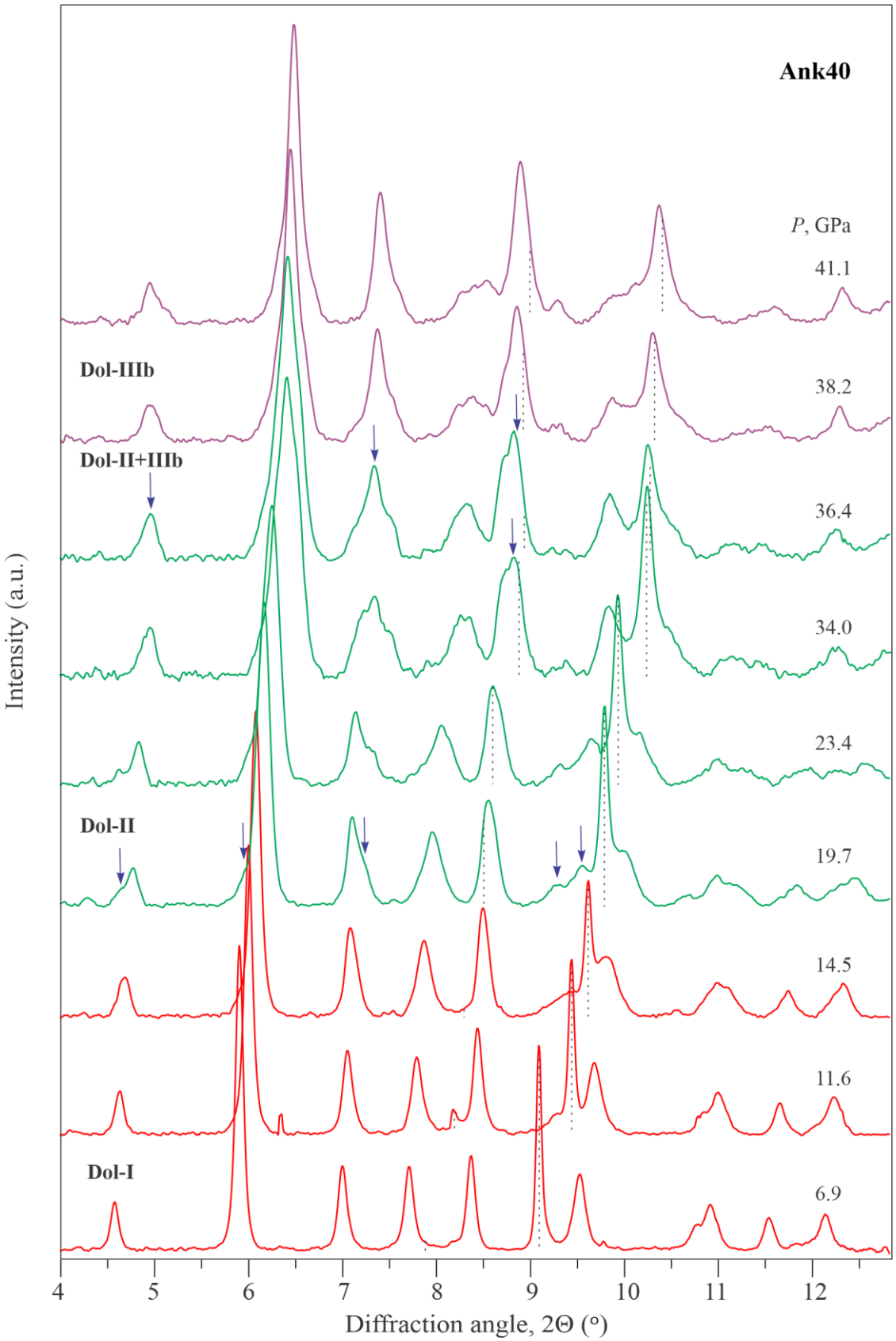

Fig. S10 The XRD patterns of Ank40 (*xFe* = 0.40) collected at different pressures. Dashed lines show the position of Ne peak. Arrows point at the new peaks.

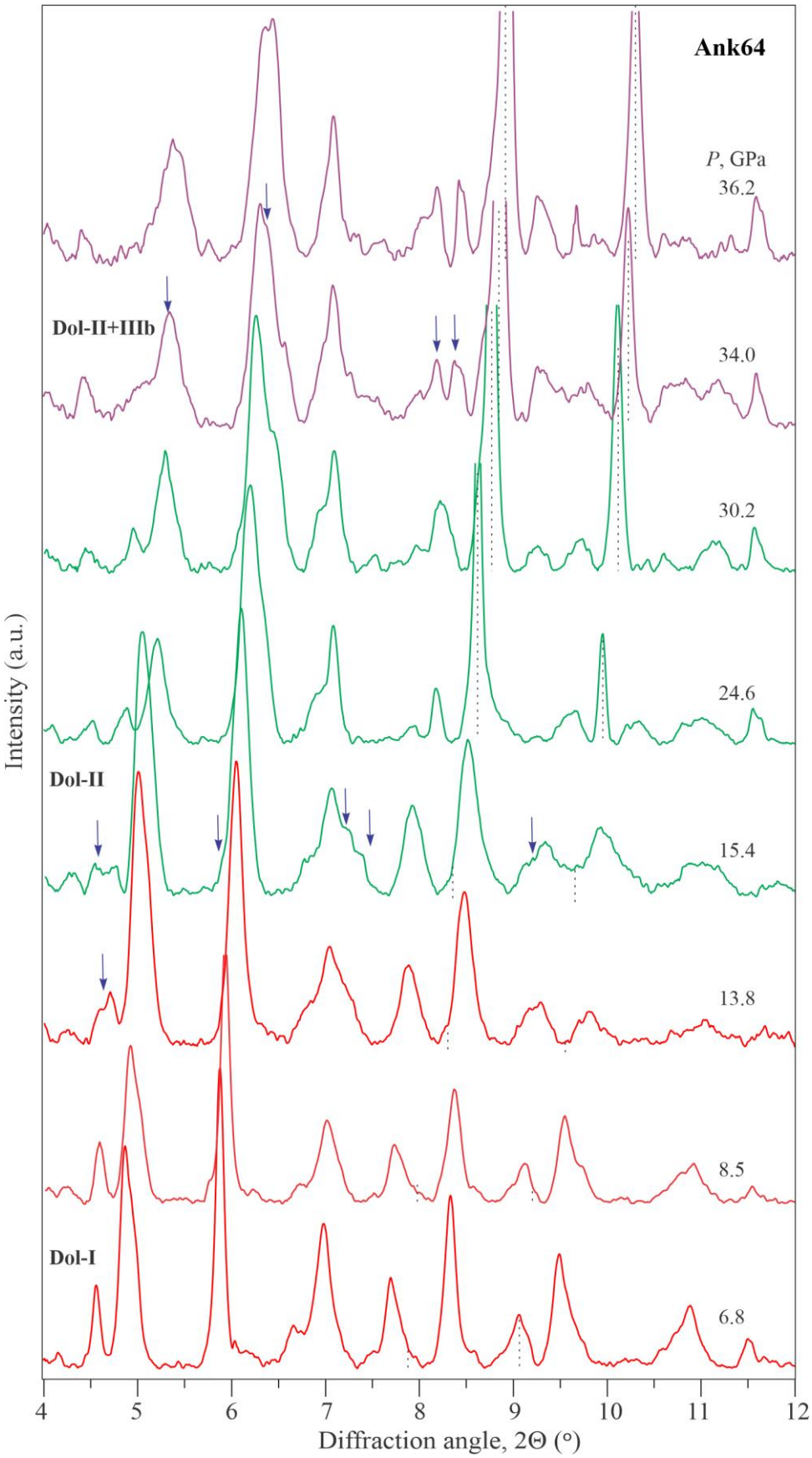

Fig. S11 The XRD patterns of Ank64 (*xFe* = 0.64) collected at different pressures. Dashed lines show position of Ne peak. Arrows point at the new peaks.

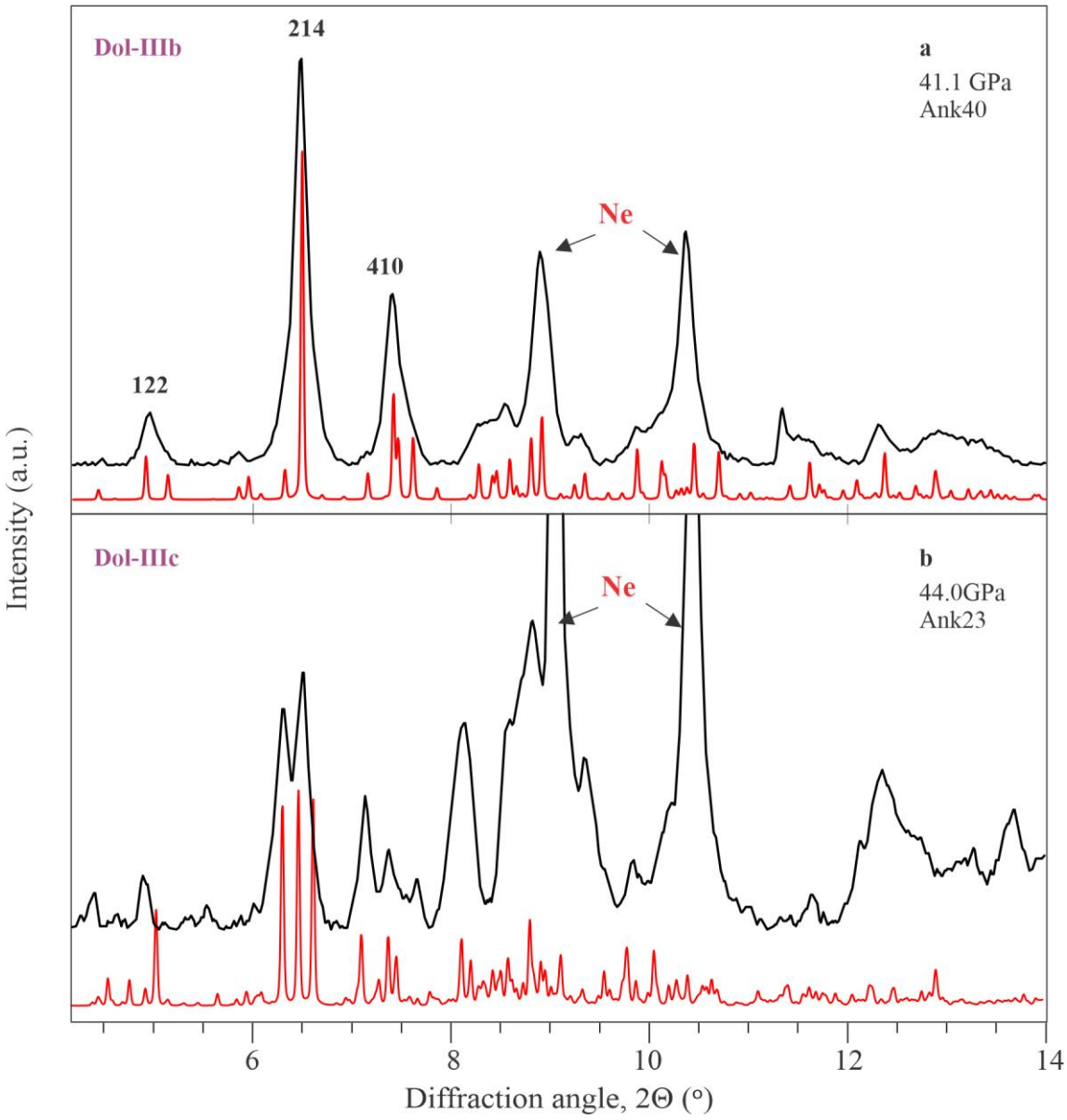

Fig. S12 The XRD patterns of Ank40 and Ank23. Calculated XRD of Dol-IIIc and IIIb (red patterns) are given for comparison.

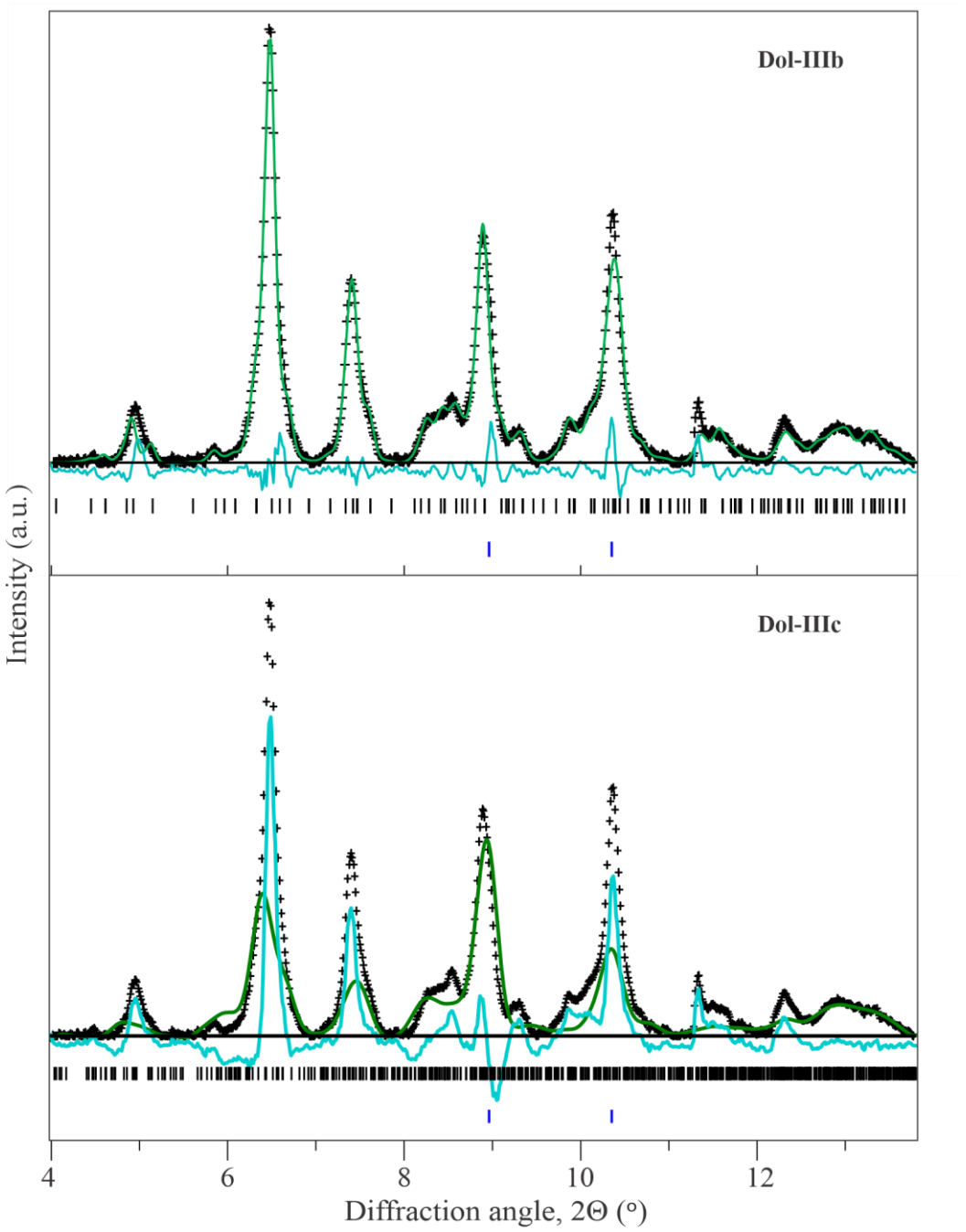

Fig. S13 The Rietveld refinement of the Ank40 XRD pattern obtained at 41.1 GPa, using Dol-IIIb (upper figure, wR=19.9%) and Dol-IIIc (lower figure, wR=42.5%) models in combination with Ne. The experimental curve is indicated with crosses. The green and blue lines represent the calculated XRD and the difference curve, respectively. The Bragg positions of Dol-IIIb or IIIc (in black) and Ne (in blue) are marked by ticks.

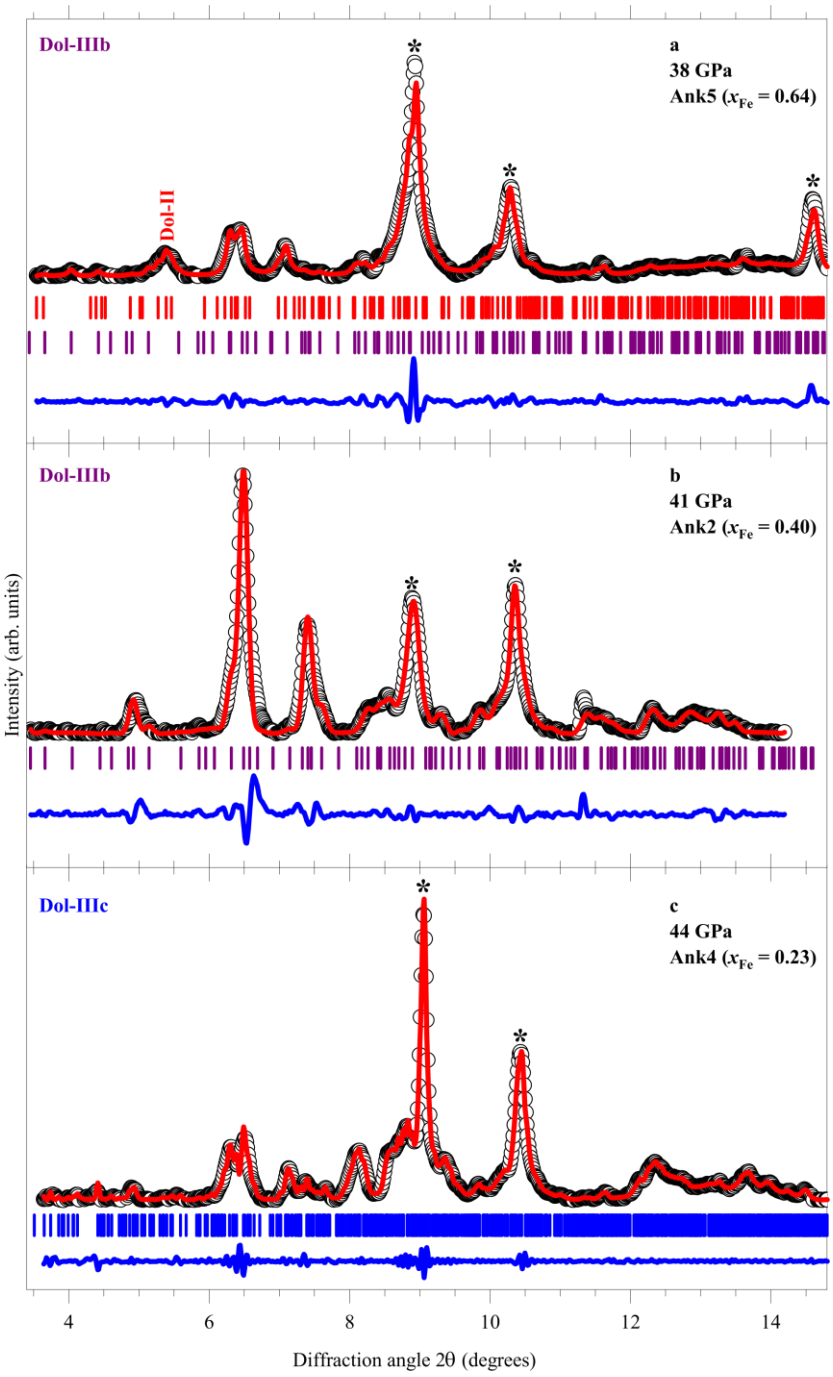

Fig. 14. The Le Bail refinements of the XRD patterns of the (a) Ank5 (P = 38 GPa), (b) Ank2 (P = 41 GPa), and (c) Ank4 (P = 44 GPa), collected at the highest experimental pressure of each run (λ = 0.2906 Å, T = 300 K). Open circles are the experimental data, red lines – the Le Bail refinements, and blue lines – the difference curves. The corresponding structural parameters are listed in Table 1. Asterisks mark the Bragg peaks of the Ne PM.

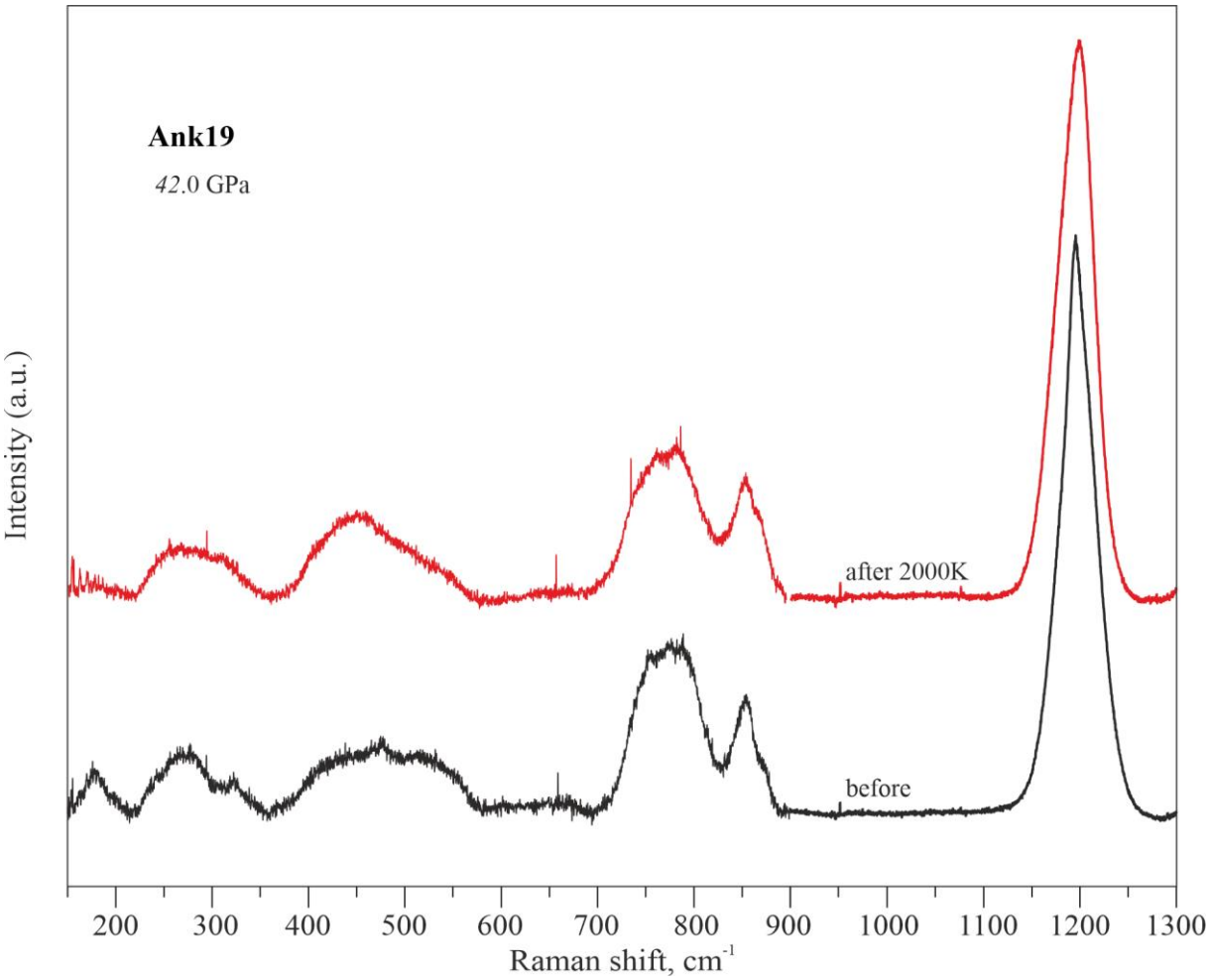

Fig. S15. Results of the Raman spectroscopy analyses of the Ank19 before and after heating at 42 GPa.